

ORIGINAL ARTICLE



Seismic response of a steel resilient frame equipped with self-centering column bases with friction devices

Elena Elettore¹, Fabio Freddi², Massimo Latour¹, Gianvittorio Rizzano¹

Correspondence

Elena Elettore
PhD Student
Department of Civil Engineering
University of Salerno
Via Giovanni Paolo II
84084 Fisciano (SA)
Email: eelettore@unisa.it

Affiliations

¹University of Salerno, Salerno, Italy.

²University College London, London, UK.

Abstract

In the last two decades many researchers focused on the development of innovative building structures with the aim of achieving seismic resilience. Among others, steel Moment Resisting Frames (MRFs) equipped with friction devices in beam-to-column joints have emerged as an effective solution able to dissipate the seismic input energy while also ensuring the damage-free behaviour of the system. However, to date, little attention has been paid to their column bases, which represent fundamental components in order to achieve resilience. In fact, column bases designed by current conventional approaches lead to significant seismic damage and residual drifts leading to difficult-to-repair structures. The present paper evaluates the seismic performance of steel MRFs equipped with an innovative damage-free, self-centring, rocking column base joints. The proposed column base consists of a rocking splice joint where the seismic behaviour is controlled by a combination of friction devices, providing energy dissipation capacity, and pre-loaded threaded bars with disk springs, introducing restoring forces in the joint. The design procedure of the column base is presented, a numerical OpenSees model is developed to simulate the seismic response of a perimeter seismic-resistant frame, including the hysteretic behaviour of the connection. Non-linear dynamic analyses have been carried out on a set of ground motions records to investigate the effectiveness of the column base in protecting the first storey columns from yielding and in reducing the residual storey drifts. Incremental Dynamic Analyses are used to investigate the influence of the record-to-record variability and to derive fragility curves for the whole structure and for several local engineering demand parameters of the frame and of the column base connection. The results show that the damage-free behaviour of the column bases is a key requirement when self-centering of MRFs is a design objective.

Keywords

Structural Resilience, Damage-free, Self-centering, Moment Resisting Steel frames, Column bases, Seismic design, Residual drifts.

1 Introduction

In the last two decades, many research studies focused on the development of seismic design methods with the aim to improve the seismic performance of building structures. According to modern seismic design codes, structures must be designed to remain elastic or only slightly damaged in case of 'frequent' (low intensity) seismic events (*i.e.*, Damage Limit State). Differently, in case of 'rare' (high intensity) seismic events (*i.e.*, Ultimate Limit State) extensive damage is generally accepted. For this latter case, structures are typically designed to concentrate the seismic damage into specific zones, referred to as plastic hinges, whose ductility and energy dissipation capacity is properly designed through the adoption of specific detailing rules. At the same time, global ductility is achieved by capacity design rules with the aim of avoiding non ductile local failures and allowing the development of a global type collapse mechanism. In steel Moment Resisting Frames (MRFs), this strategy results in over-strengthened columns and connections leading to structures characterized by weak beams and column requirements of the seismic codes, however, under high intensity events, it leads to large economic losses. In fact, being the dissipative zones

part of the main structural elements, after a destructive seismic event, the structure is often significantly damaged and characterized by large residual drifts. This implies high direct (*i.e.*, repair costs) and indirect (*i.e.*, business interruption) losses, which, in many cases, are not acceptable from both the social and economic prospective.

To overcome these drawbacks, in the last decades, many research works focused on the development of innovative structural systems, where the seismic damage is limited to easy to replace, or repair, dissipative fuses, promoting structural resilience. In the last few years, several works focused on the definition of innovative damage-free steel column bases [*e.g.*, 1-8]. Amongst others, McRae *et al.* [4] proposed two column base typologies, based on the Sliding Hinge Joint concept [5], able to provide energy dissipation capacity and, at the same time, prevent column yielding. Freddi *et al.* [6] presented a rocking damage-free steel column base in which the dissipation of the seismic energy is provided by Friction Devices (FDs) and the rocking behaviour is controlled by high-strength steel post-tensioned (PT) bars. Simple analytical equations were used to describe the monotonic and cyclic moment-rotation behaviour while non-linear dynamic analyses were carried out to show the potential of the

column base in preventing the first-floor column yielding and in eliminating the first storey residual drift. Similarly, Kamperidis *et al.* [7] proposed a partial strength low-damage self-centering steel column base equipped with PT tendons to achieve self-centering behaviour and hour-glass shape steel yielding devices, referred to as web hour-glass pins to dissipate the seismic energy. More recently, Latour *et al.* [8] proposed and experimentally investigated, an innovative rocking splice connection where the seismic behaviour is controlled by a combination of FDs and PT bars with disk springs. The FDs are realized slotting the upper part of the column above the splice, adding cover plates and friction pads pre-stressed with high strength pre-loadable bolts on both web and flanges. In this way, the alternate slippage of the surfaces in contact, on which a transversal force is applied by means of high strength bolts, dissipates the seismic energy. Conversely, the PT bars are introduced to provide restoring forces promoting the self-centering behaviour of the column base. The experimental tests demonstrated the damage-free and self-centering capabilities of this innovative column connection.

The present work numerically investigates and compares the seismic response of a traditional steel MRF with full strength column base connections and an equivalent frame structure equipped with the innovative column base connection (MRF-CB) experimentally investigated by Latour *et al.* [8]. In both cases the beam-to-column joints are conventional full-strength welded joints and the design is performed in accordance with the Eurocodes [9, 10]. The main aim of the study is to assess the structural self-centering capabilities of the two systems and to evaluate the beneficial effects provided by the introduction of the innovative column base joint in reducing residual drifts after severe seismic events. It is worth mentioning that the introduction of the proposed column base connections has a negligible influence on the overall cost of the structure.

In the following sections a case study structure is examined, addressing first the design of the column bases and then the seismic response of the two configurations. Non-linear time history analyses (NTHAs) have been carried out to investigate the effectiveness of the column base in protecting the first storey columns from yielding and reducing the residual storey drifts. To generate fragility curves, Incremental Dynamic Analyses [11] are performed, by subjecting the system to a set of 30 ground motions records for increasing values of the seismic intensity measure (IM). This procedure allows to investigate how the uncertainty affecting the earthquake input, *i.e.*, the record-to-record variability, is propagated through the structure. Has been demonstrated that, the effects of model parameter uncertainty and epistemic uncertainty are less notable than the effects of record-to-record variability [12,13] and they are not considered in this study.

Fragility curves show how the introduction of the column bases significantly contributes to the reduction of the residual interstorey drifts for the seismic intensities of interests. In addition, fragility curves are derived for several components of the frame and of the column base connection by using both global and local engineering demand parameters, as suggested in [14, 15, 16]. To this aim, interstorey drift limits are correlated to member-level limits, *e.g.*, ultimate chord rotation capacity of members, through a pushover analysis and then are used as EDPs in the probabilistic study. The comparison of the components' fragility curves indicates how the introduction of the column bases protects beams and columns from reaching their ultimate rotation capacity and provide information on the hierarchy of activation of different mechanisms within the structure.

2 Case study frame

The considered case study structure is a 4-storey building with 5 bays in

-x direction and 3 bays in -y direction. The considered layout has inter-storey heights of 3.20 m except for the first level, whose height is equal to 3.50 m, while all the bays have spans of 6 m. Seismic resistant perimeter MRFs are located in the -x direction. Plan and elevation views of the case study frame are reported in Fig. 1. The case study frame is designed according to the Eurocode 8 [10]. The Type 1 elastic response spectrum with a peak ground acceleration equal to 0.35g and soil type C is considered for the definition of the Design Based Earthquake (*i.e.*, DBE, probability of exceedance of 10% in 50 years). The building has non-structural elements fixed in a way so as not to interfere with structural deformations, and therefore, the interstorey drift limit for the damage limitation requirements (*i.e.*, probability of exceedance of 10% in 10 years) is assumed as 1%. The maximum credible earthquake (MCE) is assumed to have intensity equal to 150% the DBE. The steel yield strength is equal to 355 MPa for the columns, 275 MPa for beams, and 900 MPa for the PT bars. The selected profiles are IPE 550 and IPE 500 for beams, while HE 600B and HE 500B for columns of the first and the last two stories, respectively. The study focuses on the assessment of the seismic resisting frame in the -x direction, where the MRFs are employed.

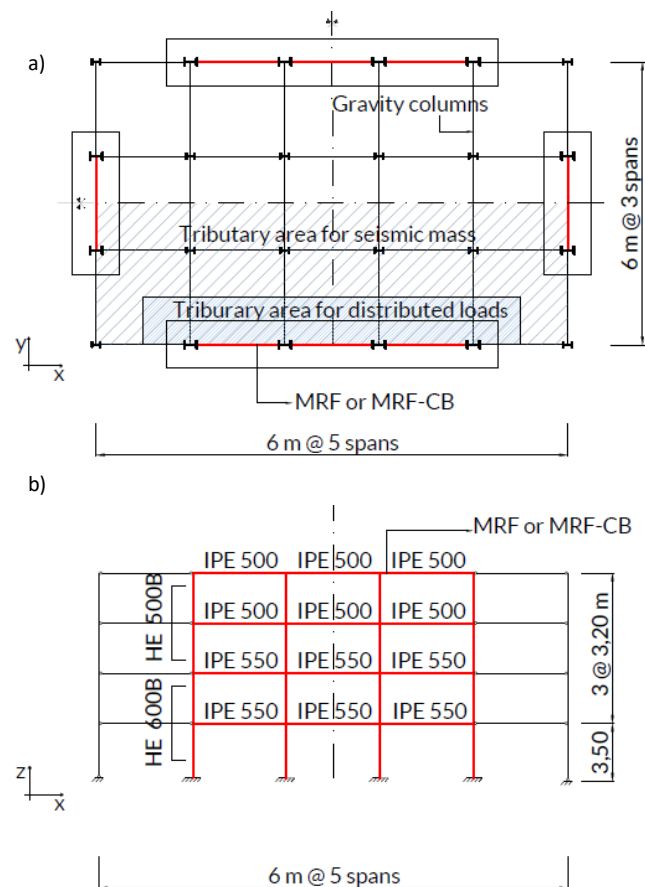


Figure 1 (a) Plan view and (b) Elevation view of the case study building.

3 Column base connection design

The investigated column base connection [8] consists in a slotted column splice equipped with FDs assuring the seismic input energy dissipation capacity and PT bars with disk springs to introduce restoring forces in the joint, granting the self-centering behaviour. An overview of the investigated connection is reported in Fig. 2 and additional details are reported in [17]. The cyclic behaviour of FDs is characterized by a rigid-plastic hysteretic model, which depends on the clamping force and on the friction coefficient μ of the contact interfaces. The self-centering behaviour is granted by a system composed of PT bars and disk springs arranged in series as a macro-spring element able to ensure a sufficient deformability to the connection and providing restoring forces to return towards the initial straight position at the end of the seismic event. To hold these

bars, plates, designed to withstand the self-centering force in elastic range, are welded to the column. In order to allow the gap opening, the holes are designed to accommodate a minimum rotation of 40 mrad which is the benchmark rotation established by [18], for Special MRFs.

3.1 Structural details

According to design requirements of the Eurocodes, under both gravity and seismic loads, the first storey columns have sections HEB600 made of S355 steel. The column base is constituted by two parts, connected using S355 steel plates, fastened by HV M30 10.9 class bolts to the web and flanges, applied in both outer and inner parts of the column. Friction pads consist of 8 mm thermally sprayed friction metal steel shims placed between the steel plates and the column. Figure 2 shows a 3D view of the proposed column base connection and the required components.

3.2 Moment-rotation behaviour

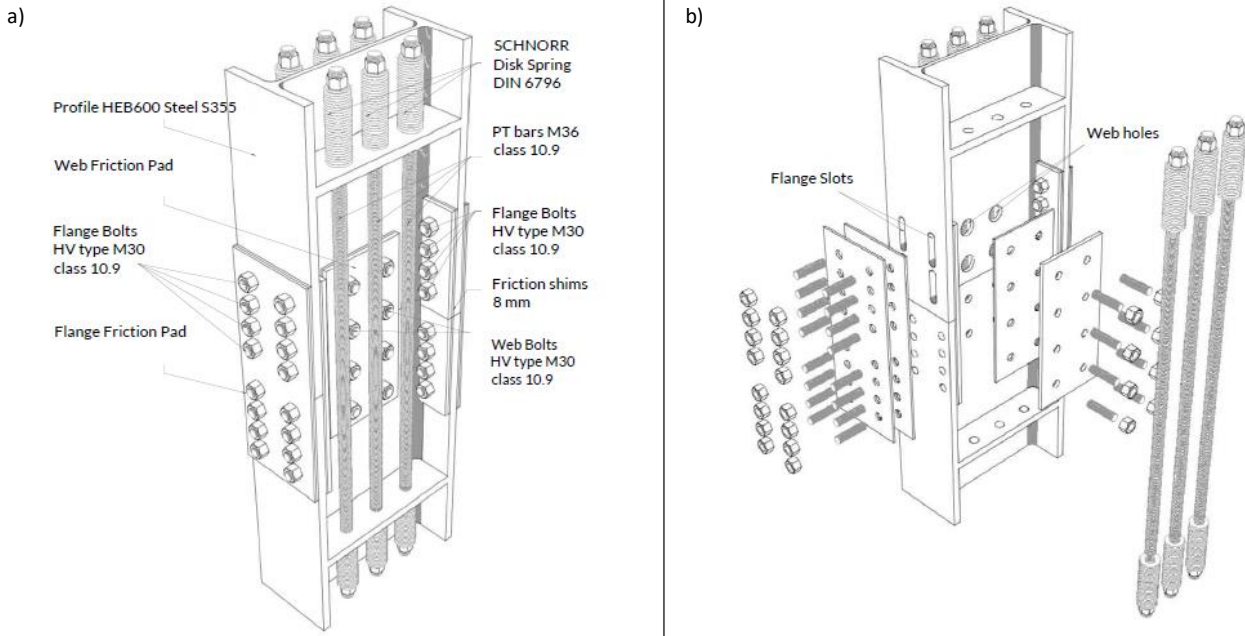


Figure 2 Details of the proposed column base connection: (a) 3D view; (b) Exploded 3D view.

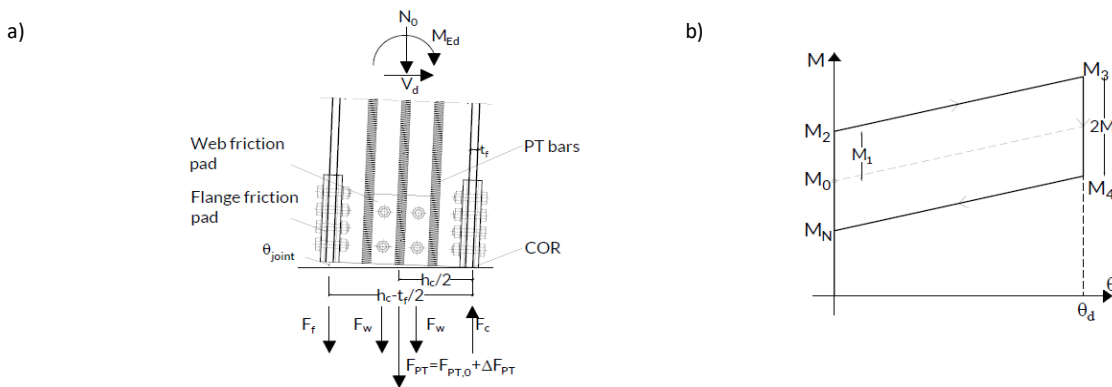


Figure 3 Behaviour of the column base connection. (a) Force interaction among the components during the gap-opening; (b) Theoretical moment-rotation relationship

M_1 represents the contribution to the bending moment due to FDs and is equal to:

The expected forces in each component during the rocking behaviour can be represented by imposing static equilibrium at the centre of rotation (COR) as reported in Figure 3(a). F_w and F_f represent the forces in the friction pads on the column web and flange respectively, while F_{PT} represents the sum of the forces provided by the threaded bars with disk springs. F_{PT} represents the post-tensioning forces while ΔF_{PT} represents the additional forces as consequence of the gap opening. The moment-rotation behaviour of the column base connection is function of the response of each component and can be represented by the flag-shape curve of Figure 3.

M_0 corresponds to the decompression moment due to the sum of the moment contributions related to the gravity loads directly applied on the structure (M_N) plus the moment provided by the PT bars at zero rotation ($M_{PT,0}$). M_0 can be calculated as follows:

$$M_0 = (N_0 + F_{PT,0}) \frac{h_c}{2} \quad (1)$$

where N_0 is the axial load applied to the joint section, $F_{PT,0}$ is the sum of the initial post-tensioning forces of the PT bars and h_c is the height of the column's section.

$$M_1 = F_f \left(h_c - \frac{t_{fc}}{2} \right) + F_w \frac{h_c}{2} \quad (2)$$

where F_r and F_w represent the sliding force in the friction pads of the column flanges and web. M_2 is the moment that initiate the gap opening and is given by the sum of M_0 and M_1 while M_3 is the maximum moment achieved at the design rotation $\theta_d = 0,04$ rad. Its value is determined by accounting for the additional forces in the PT bars as consequence of the gap opening:

$$M_3 = M_0 + M_1 + (K_{eq} \theta_{joint} \frac{h_c}{2}) \frac{h_c}{2} \quad (3)$$

K_{eq} is the rotational stiffness of the whole system, which can be determined as follows:

$$K_{eq} = \frac{K_{PT} K_{ds}}{K_{PT} + K_{ds}} \quad (4)$$

$$K_{PT} = \frac{n_b E_{pt} A_{pt}}{l_{pt} + l_{ds}} \quad K_{ds} = \frac{K_{ds1} n_{par}}{n_{ser}} \quad (5)$$

where n_b is the number of bars employed in the connection symmetrically placed with respect to the column centre, $l_{pt} + l_{ds}$ is the bars length considering the total length of the disk spring system, n_{par} and n_{ser} are the number of disk springs in parallel and in series respectively and K_{ds1} is the stiffness of the single disk spring. It is important to stress that the maximum moment M_3 , must be lower than the yielding moment of the column to avoid damage. Based on these equations, the self-centering behaviour of the connection if achieved if the moment generated by the axial components (M_0), is higher than the moment provided by the FDs (M_1).

The design actions for column base connection considered for case study purposes, are derived based on the seismic analysis of the equivalent frame with rigid full-strength column bases. The column axial load N_0 is assumed equal to the combination of the compression force due to the non-seismic actions ($N_{Ed,G}$) and the axial load in the column due to the design seismic action ($N_{Ed,E}$); as required by the Eurocode 8 [10] (§6.6.3) (*i.e.*, $N_{Ed} = N_{Ed,G} + 1.1 \gamma_{ov} \Omega N_{Ed,E}$) and is equal to $N_{0,int} = 460$ kN and $N_{0,ext} = -807$ kN for the inner and outer column respectively. The columns' bending moment is calculated considering the most unfavourable combination of axial forces and bending moments as required by the Eurocode 8 [10] (§6.6.3) (*i.e.*, $M_{Ed} = M_{Ed,G} + 1.1 \gamma_{ov} \Omega M_{Ed,E}$). The design bending moments are defined considering the proper location of the column splices and have been set respectively equal to $M_{Ed,int} = 1985$ kNm and $M_{Ed,ext} = 1633$ kNm for the inner and outer columns. Finally, the shear force is computed as $V_d = M_{Ed}/L_0$, where L_0 is the shear length. Hence, the shear force is equal to $V_{d,int} = 894$ kN and $V_{d,ext} = 605$ kN for the inner and outer column. The properties of the column base connections obtained by the design for the inner and outer column are reported in Table 1.

4 Structural modelling

4.1 Frame modelling

2-D non-linear finite element (FE) models of the frames are developed in OpenSees [19]. Beams are modelled by a lumped plasticity approach where plastic hinges are described by zero-length non-linear rotational springs at beams' ends following a bilinear hysteretic rule based on the modified Ibarra-Krawinkler deterioration rule as suggested by Lignos and Krawinkler [20]. Conversely, in order to capture the axial force-bending moment interaction, columns are modelled by the distributed plasticity approach with 4 integration points. The 'Steel01' material [1] for 355 MPa yield strength and 0.2% post-yield stiffness ratio is employed. At the beam-column connections, the panel zone is modelled with the 'Scissor' model [21]. The panel area of the column is stiffened with doubler plates, to promote the plastic engagement of the beams only. The rigid-floor diaphragm is modelled by assigning a high value to the axial stiffness to the beams. Gravity loads are applied on the beams by considering the seismic combination of the Eurocode 8 [10], while the masses are concentrated at the beam-column connections. Damping sources other than the hysteretic energy dissipation are modelled through the Rayleigh damping matrix where the values of the mass-related and stiffness-related damping coefficients are considered for a damping factor of 2% for the first two vibration modes. Additional details on the modelling approach are provided in Elettore *et al.* [17].

4.2 Column Base Modelling

A 2-D FE model of the proposed column base is developed in OpenSees [19] as reported in Figure 4. The column is modelled with non-linear force-based fibre elements associated with the 'Steel01' material [19] for 355 MPa yield strength and 0.2% post-yield stiffness ratio. The rigid elements of the rocking interface are modelled with 'Elastic beam-column' elements with very high flexural stiffness and are used to connect the lower and the upper part of the column through non-linear springs. These springs are represented by four bilinear 'zero-length' elements in parallel with gap elements to simulate the bilinear hysteretic response of the FDs and the contact behaviour of the column interfaces. FDs for both flanges and web are modelled by the 'Steel01' material considering a very high initial stiffness and very low post-elastic stiffness in order to model the rigid plastic behaviour of the FDs. Conversely, the contacts elements are defined by the 'Elastic compression-no tension' (ENT) material, which exhibits an elastic compression-no tension force-displacement behaviour. The compression stiffness of the contact spring is assumed equal to 10 times the axial stiffness of the column. Additionally, a central 'Zero-length' translational spring with bilinear elastic-plastic behaviour is used to model the force provided by PT bars with disk springs. In this case, being symmetrically placed, the six PT bars can be modelled by a single central spring with the stiffness of the whole system. The initial post-tensioning force is modelled by imposing an initial strain equal to $F_{PT}/A_{PT}E_{PT}$ by using the 'Initial strain material' along with the elastoplastic material 'Steel01'. A comparison of the numerical and experimental results is carried out and is reported in [17].

Table 1. Material properties of the column base connections

| Elements | Material properties | | | | Outer column | | Inner column | |
|---------------------|---------------------|--------------|------------------|------------------|--------------|--------------------|--------------|--------------------|
| | Class | E [GPa] | f_y [MPa] | f_u [MPa] | number | Pre-load [kN] | number | Pre-load [kN] |
| Column and plates | S355 | 210 | 355 | 510 | - | - | - | - |
| Post-tensioned bars | 10.9 | 205 | 900 | 1000 | 8 | 570 | 6 | 570 |
| Web Bolts | 10.9 | 210 | 900 | 1000 | 4 | 140 | 4 | 210 |
| Flange Bolts | 10.9 | 210 | 900 | 1000 | 8 | 60 | 8 | 110 |

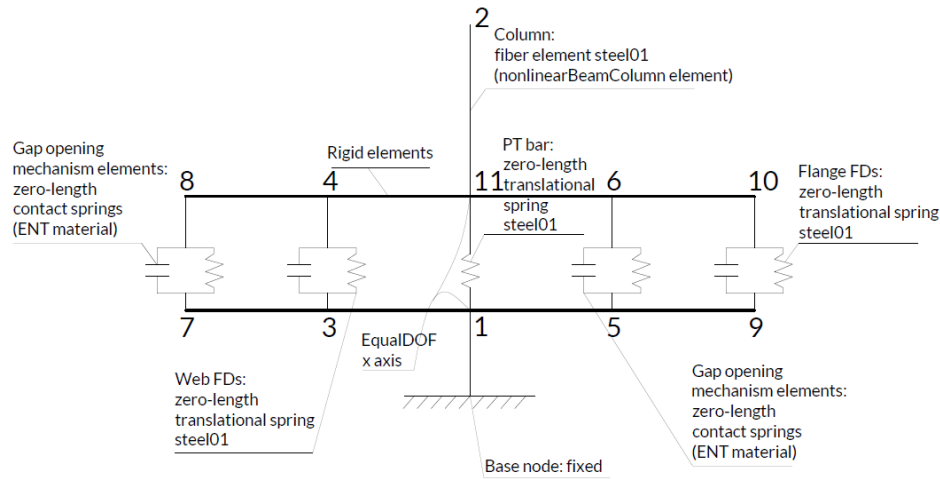


Figure 4 Two dimensional OpenSees model of the column base connection

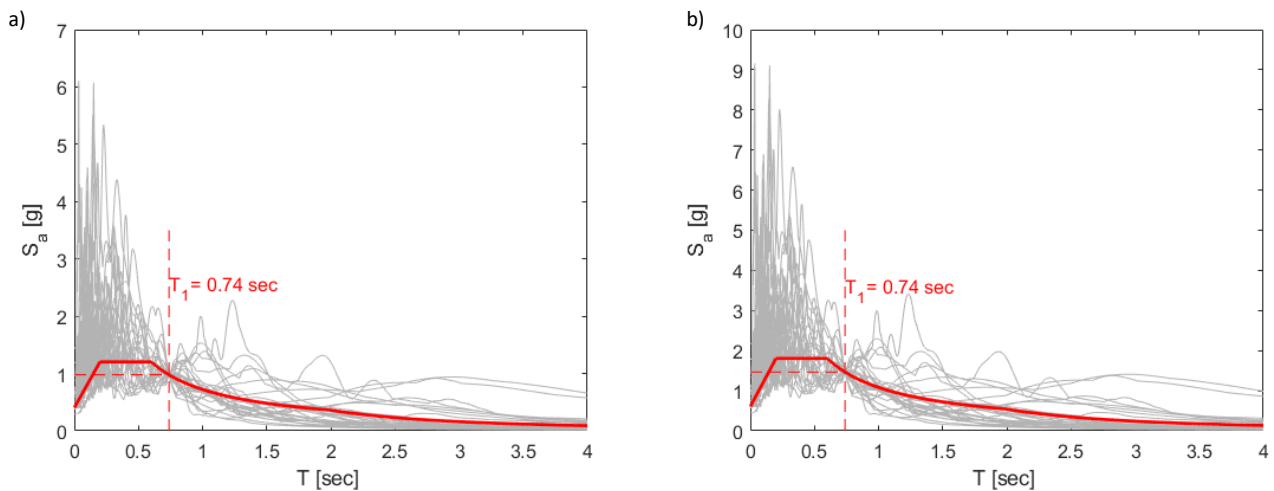


Figure 5 Set of 30 scaled GMs for the two structures having the same period of vibration ($T_1 = 0.74s$); (a) DBE and (b) MCE intensities

5 Performance-based assessment

NLTHAs are performed in order to assess how the proposed column base influences the seismic response of the frame and Incremental Dynamic Analyses (IDAs) [11] are used to assess the influence of the record-to-record variability. The MRF and the MRF-CB are analysed, and the results compared. The fundamental period of vibration $T_1 = 0.74$ sec is the same for both the structures and the spectral acceleration corresponding to T_1 ($S_a(T_1)$) is used as intensity measure (IM). A set of 30 natural ground motions (GMs) records are selected from the SIMBAD Database [22] and scaled to increasing values of IM to cover the whole range from elastic to non-linear seismic response up to collapse in order to perform the IDAs. Figure 5 shows the spectra for the 30 earthquake GMs scaled to the DBE ($S_a = 0.98g$) and MCE ($S_a = 1.46g$) seismic intensities defined considering an inherent damping ratio of 2%.

Global parameters are recorded allowing the comparison of the seismic performance of the two systems. It can be observed that, despite a self-centering system is present only at the first storey, the introduction of the proposed column bases allows a reduction of the residual drifts on the whole structure. Both for the DBE and the MCE, the MRF-CB experiences values of residual drifts lower than 0.5%, often considered the threshold beyond which repair of the building may not be economically viable [23]. This limit is not satisfied at MCE for the structure with full-strength column bases. Moreover, it is observed that the introduction of the proposed column bases does not affect the maximum response parameters of the structure, *e.g.*, max interstorey drifts. Figures 6(a) and

(b) show respectively the comparison of the response of the two frames in terms of first storey displacements and residual drifts distribution at all the storeys considering a single GM. For the sake of brevity only the results related to one GM scaled to the MCE intensity are reported here.

The response of local EDPs have been also investigated in order to provide a better understanding of the components' behaviour. It is also observed that in both structures, beams develop plastic hinges, columns remain elastic due to the capacity design rule enforced during the design according to the Eurocode 8, the bottom sections of the first storey columns yield in the MRF with conventional base connections while remain elastic range for the MRF-CB. This is expected as due to the limitation imposed on the moment capacity of the connection during the design. Additionally, webs and flanges of the panel zones remain within the elastic range for both the structures thanks to the introduction of the doubler plates.

The results of the IDA for the residual and peak interstorey drifts (IDR) are shown in Figures 7 for the first and fourth storey and demonstrate what observed from the results of the single GM. The record-to-record variability significantly affect the results in terms of residual drifts, as expected and as demonstrated by several studies focusing on this topic. However, it is possible to observe that the introduction of the column bases is beneficial also in reducing the uncertainty of this response parameter.

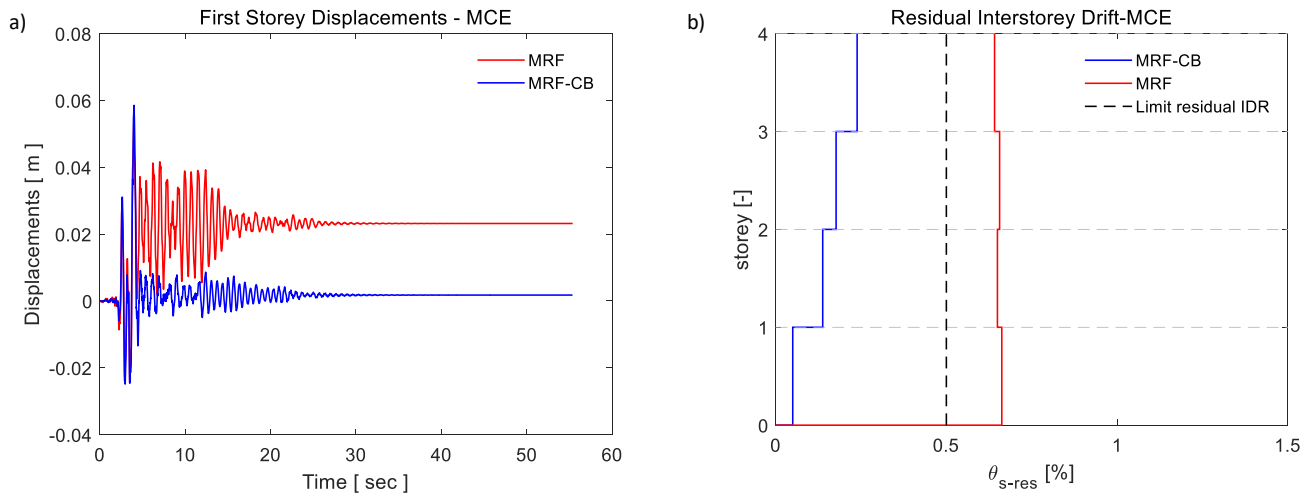


Figure 6 1st storey displacement time history for (a) DBE and (b) MCE intensities.

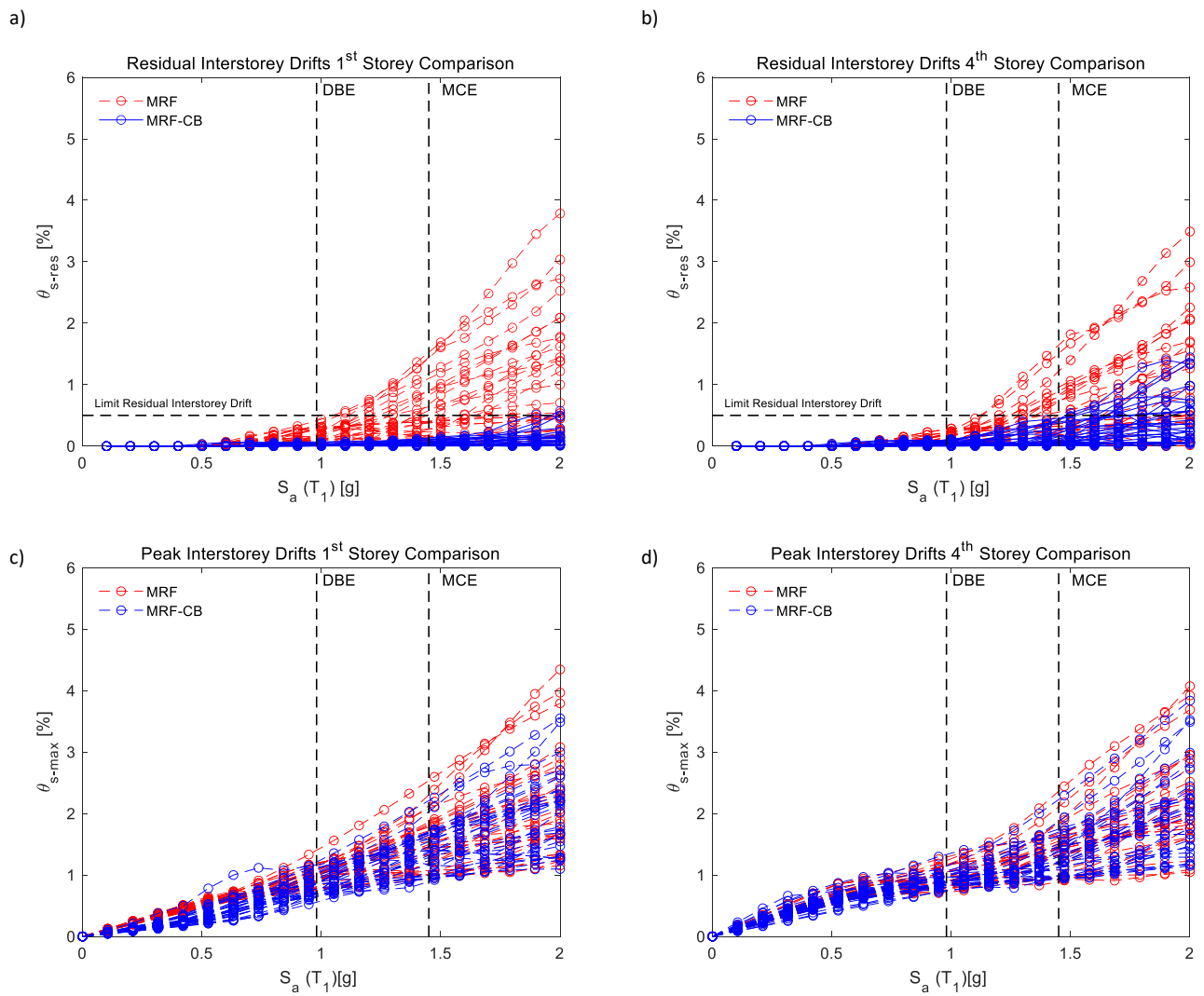


Figure 7 IDA comparison of the results MRF – MRF-CB

The performances of the two structures are presented in terms of fragility curves, using the results of the Incremental Dynamic Analyses. Results show how the introduction of the column bases significantly contributes to the reduction of the residual interstorey drifts for the seismic intensities of interests, as described in the Figure 8.

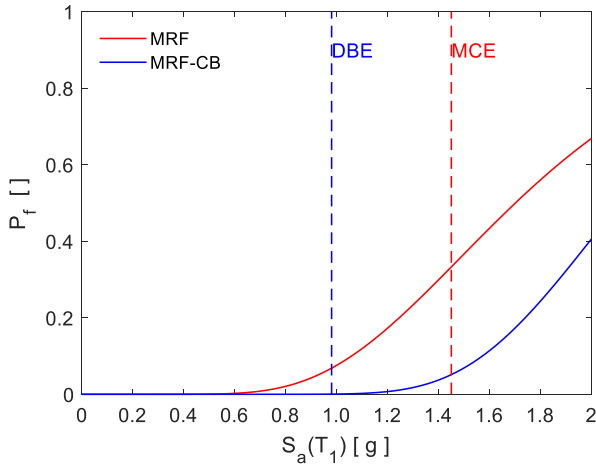


Figure 8 Fragility curves comparison for residual interstorey drift

5.1 Component Fragility Curves

Components fragility curves are derived following the mapping between local and global EDPs defined by pushover analysis. The interstorey drift limits are derived from the member-level limits, following the approach suggested in [12], with the aim of considering specific member detailing. Standard pushover analyses with a distribution of lateral forces defined according to the first mode shape are performed in order to relate local

and global EDPs and to calibrate the maximum interstorey drift thresholds mapping. Different member-level criteria are selected considering the specific member-level performances for the MRF with conventional column bases (e.g., ultimate chord rotation capacity of members) and for the MRF-CB, including the column bases components (e.g., sliding of the friction devices, yielding of the PT bars). The drift limits are compared using the global-level drift limits for each performance level (Slight, Moderate, Extensive, Collapse), which are defined for Steel Moment Frames according to [24]. The drift limits corresponding to the member-level criteria are summarized in Table 2 and, for the sake of brevity, only the minimum limits which correspond to the interstorey drifts of the first storey, are reported.

Figure 9 shows the results of the pushover analyses by showing the storey shear versus the interstorey drift for each storey of the two structures. It is important to stress that the capacity for local EDPs at the other storeys is reached for similar values of interstorey drifts as expected from the design.

Based on these threshold values, expressed in terms of interstorey drifts but related the failures at components level, fragility curves are derived and compared. The comparison of the fragility curves of the different components within the same structure and of the same components between the two structures provide useful insights. First of all, it can be observed the hierarchy of activation of different mechanisms within the structure. The beams are the first to yield in all storeys and both the structures. This highlight that the introduction of the column bases does not protect the beams from yielding as expected from the design. However, following the yielding of the beams the friction devices in the column bases are activated. The comparison of the fragility curves in Figures 10(a) and (b) indicates how the introduction of the column bases do not produce any detrimental effect on the other components.

Table 2 Interstorey drifts limits based on DSs thresholds mapping

| Damage Level | | MRF | MRF-CB | HAZUS |
|--------------------|---|-------|--------|-------|
| $M_{el,b}$ | Limit of elastic behaviour in one beam | 4.1 ‰ | 4.0 ‰ | 4.0 ‰ |
| $M_{pl,b}$ | Yielding in one beam | 5.3 ‰ | 5.2 ‰ | 8.0 ‰ |
| FDs | Sliding force of the friction devices | - | 6.7 ‰ | 8.0 ‰ |
| $\vartheta_{u,b}$ | Ultimate chord rotation $\vartheta_{u,b}$ in one beam | 3.1% | 3.0 % | 2.5 % |
| $M_{pl,c}$ | Yielding in one column | 4.2% | - | 5.0 % |
| $\vartheta_{u,CB}$ | Ultimate chord rotation $\vartheta_{u,CB}$ of the CB | - | 4.7 % | 5.0 % |
| PT_y | Yielding of the PT bar | - | 6.0 % | - |

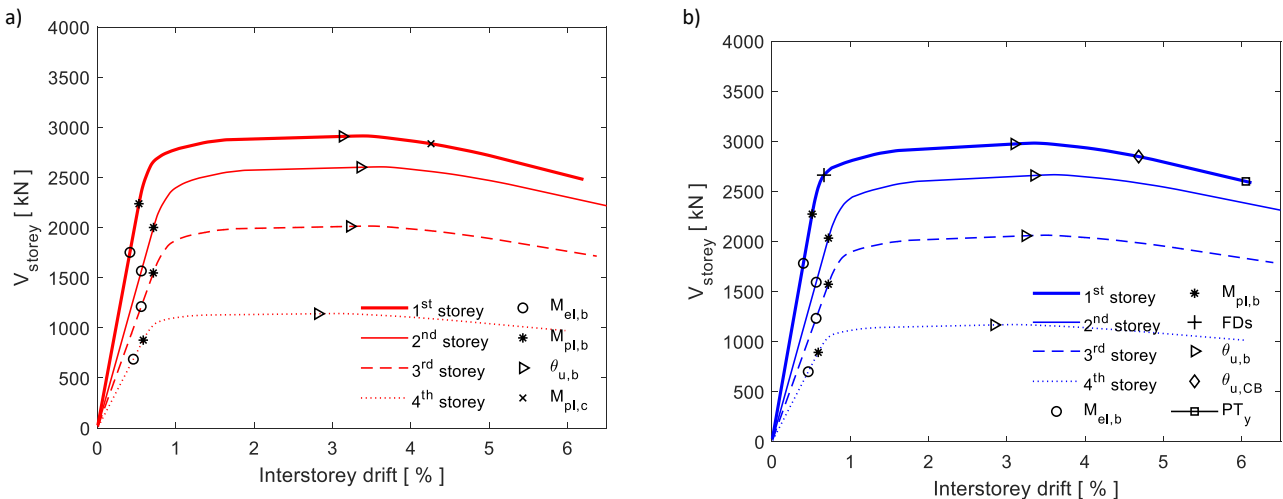


Figure 9 Pushover curves and damage state thresholds for the MRF (a) and MRF-CB (b).

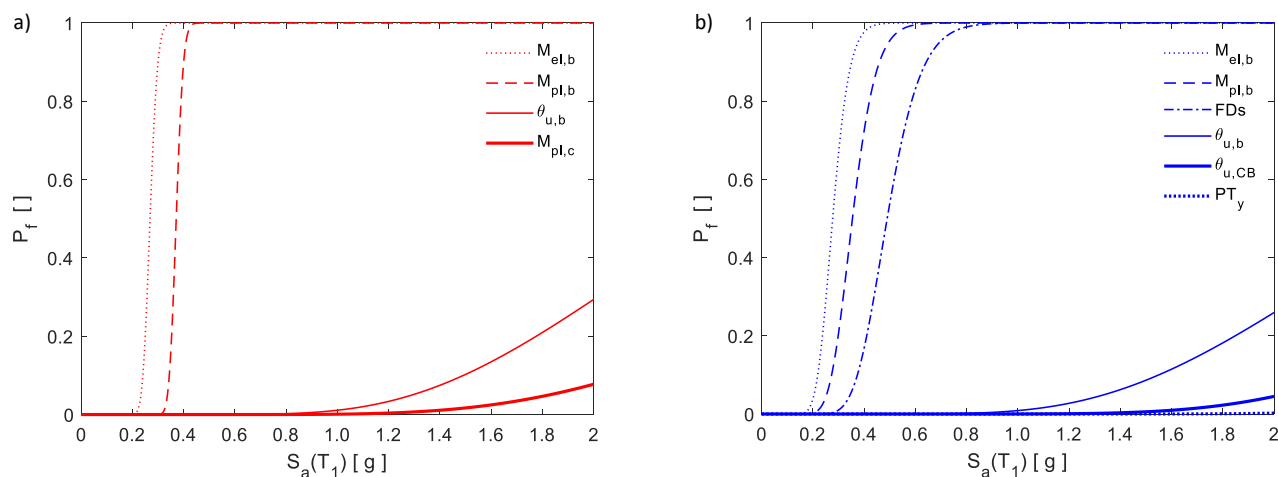


Figure 10 Fragility curves and damage state thresholds for the MRF (a) and MRF-CB (b).

6 Summary and conclusion

This work investigates the behaviour of an innovative column base connection composed of a rocking splice joint where the seismic behaviour is controlled by a combination of friction devices that promote the energy dissipation and the post-tensioned bars introduced to provide self-centering capabilities to the column base. A case study structure is examined, addressing first the design of the column bases and then the seismic response of the two configurations. Non-linear dynamic analyses are performed on the two structures to validate the effectiveness of the proposed column bases connections. The following conclusions are drawn:

- The global behaviour of the structure is significantly enhanced by the self-centering capability of the column bases in limiting residual deformations, under both the design basis and the maximum credible earthquake intensities;
- The column bases fully protect the first storey column from yielding, thus avoiding non-reparable damage, even under strong GM events;
- The comparison of the component fragility curves indicates how the introduction of the column bases do not produce any detrimental effect on the other components and provide information on the hierarchy of activation of the different mechanisms within the structure.

References

- [1] Chou, CC; Chen, JH. (2011) Analytical model validation and influence of column bases for seismic responses of steel post-tensioned self-centering MRF systems. *Engineering Structures*, 33(9):2628–2643
- [2] Chi, H; Liu, J. (2012) Seismic behavior of post-tensioned column base for steel self-centering moment resisting frame, *Journal of Constructional Steel Research*, 78:117–130
- [3] Borzouie, J; MacRae, GA; Chase, JG; Rodgers, GW; Clifton, GC. (2016) Experimental studies on cyclic performance of column base strong axis – aligned asymmetric friction connections. *Journal of Structural Engineering (ASCE)*, 142(1): 04015078–1:10
- [4] MacRae, GA; Urmson, CR; Walpole, WR; Moss, P; Hyde, K; Clifton, GC. (2009), Axial Shortening of Steel Columns in Buildings Subjected to Earthquakes, *Bulletin of The New Zealand Society for Earthquake Engineering*, 42(4): 275-287
- [5] Clifton, GC; Butterworth, JW. (2000), Moment-resisting steel framed seismic-resisting systems with semi-rigid connections, 12th World Conference on Earthquake Engineering, January 30 - February 17, Auckland, New Zealand
- [6] Freddi, F; Dimopoulos, CA; Karavasilis, TL. (2017), Rocking damage-free steel column base with friction devices: design procedure and numerical evaluation, *Earthquake Engineering and Structural Dynamics*, 46: 2281-2300
- [7] Kamperidis, V; Karavasilis, TL; Vasdravellis, G. (2018), Self-centering steel column base with metallic energy dissipation devices, *Journal of Constructional Steel Research*, 149: 14-30
- [8] Latour, M; Rizzano, G; Santiago, A; Da Silva, L. (2019), Experimental response of a low-yielding, self-centering, rocking column base joint with friction dampers, *Soil Dynamics and Earthquake Engineering*, 116: 580-592
- [9] EN 1993-1-8: 2005, Eurocode 3: Design of steel structures, Part 1-8: Design of joints. European Committee for Standardization, Brussels
- [10] EN 1998-1: 2004, Eurocode 8: Design of structures for earthquake resistance – Part 1: General rules, seismic actions and rules for buildings. European Committee for Standardization, Brussels
- [11] Vamvatsikos, D; Cornell, CA. (2002), Incremental Dynamic Analysis, *Earthquake Engineering and Structural Dynamics*, 31 (3): 491-514
- [12] Kwon, OS; Elnashai, A. (2006) The effect of material and ground motion uncertainty on the seismic vulnerability curves of RC structure. *Engineering Structures*, 28(2):289–303. DOI: 10.1016/j.engstruct.2005.07.010
- [13] Tubaldi, E; Barbato, M; Dall’Asta, A. (2012) Influence of model parameter uncertainty on seismic transverse response and vulnerability of steel-concrete composite bridges with dual load path. *Journal of Structural Engineering*; 138(3):363–374. DOI: 10.1061/(ASCE)ST.1943-541X.0000456
- [14] Hueste, MD; Bai, JW. (2006) Seismic Retrofit of a Reinforced Concrete Flat-Slab Structure: Part II – Seismic Fragility Analysis. *Engineering Structures*; 29(6):1178–1188. DOI: 10.1016/j.engstruct.2006.07.022
- [15] Freddi, F; Padgett, JE; Dall’Asta, A. (2017) Probabilistic seismic

- demand modeling of local level response parameters of an RC frame. *Bulletin of Earthquake Engineering*; 15(1): 1–23.
- [16] Freddi, F; Tubaldi, E; Ragni, L; Dall'Asta, A. (2013) Probabilistic performance assessment of low-ductility reinforced concrete frames retrofitted with dissipative braces. *Earthquake Engineering & Structural Dynamics*; 42 (7): 993–1011.
- [17] Elettore, E; Freddi, F; Latour, M; Rizzano, G. (2019), Design and Analysis of a steel seismic resilient frame equipped with self-centering column bases with friction devices, SECED conference, September 9 – 10 Greenwich, London
- [18] ANSI/AISC 341-16, Seismic provisions for structural steel buildings, Chicago, Illinois, USA
- [19] Mazzoni, S; McKenna, F; Scott, MH; Fenves, GL. (2009), OpenSEES: Open System for earthquake engineering simulation, Pacific Earthquake Engineering Research Centre (PEER), University of California, Berkeley, CA, Available at: <http://opensees.berkeley.edu>
- [20] Lignos, D; Krawinkler, H. (2011), Deterioration Modelling of Steel Components in Support of Collapse Prediction of Steel Moment Frames under Earthquake loading, *Journal of Structural Engineering*, 137: 1291-1302
- [21] Charney, F; Downs, W. (2004), Modelling procedures for panel zone deformations in moment resisting frames. *Connections in Steel Structures V. ESSC/AISC Workshop*, Amsterdam
- [22] Iervolino, V; Galasso, C; Cosenza, E. (2010), REXEL: Computer aided record selection for code-based seismic structural analysis, *Bulletin of Earthquake Engineering*, 8: 339-362
- [23] McCormick, J; Aburano, H; Nakashima, M. (2008), Permissible residual deformation levels for building structures considering both safety and human elements, *14th World Conference on Earthquake Engineering (WCEE)*, October 12-17, Beijing, China
- [24] FEMA. HAZUS-MH MR3 Technical Manual. (2003) Washington (DC): Federal Emergency Management Agency.